International Journal of
INTELLIGENT SYSTEMS AND APPLICATIONS IN ENGINEERING
ISSN:2147-6799 www.ijisae.org Original Research Paper

Contactless Vital Sign Monitoring using Radar-Based Sensors

[1]Prasad Rayi, [2]Rama Subbanna, [3]Sakthivel S, [4]Paidimalla Nagaraju

Submitted: 07/09/2024 **Revised:** 20/10/2024 **Accepted:** 29/10/2024

Abstract: Precise and ongoing surveillance of vital signs is essential for clinical decision-making, prompt intervention, and patient management. Contact-based approaches and wearable devices provide trustworthy readings; nonetheless, they encounter limits in contexts such as newborn care and burn units, as well as problems pertaining to pain, maintenance expenses, and adherence. Noncontact systems, including vision-based and Radio-Frequency (RF) methodologies, provide a possible alternative. These technologies provide vital sign monitoring without physical contact and are garnering increased interest due to advancements in sensor technology, computer vision, and machine learning, with the rising need for remote healthcare solutions. Vision-based systems excel in accurate localization but are affected by lighting conditions, while RF systems are resilient to environmental variables but need subject participation. The unique attributes of vision-based and RF-based approaches have spurred increasing interest in multi-sensory vital sign detection since 2020. This study offers a thorough summary of improvements in vision and RF modalities, together with contemporary multi-sensory techniques, to entice scholars from several disciplines to engage in multimodal fusion research on contactless vital sign detection. We delineate measuring concepts, contrast single-modality and multimodal systems, examine public datasets, assessment criteria, and cutting-edge algorithms. This study identifies the complimentary capabilities of vision and RF systems, addressing significant gaps in multimodal research and outlining future prospects from both practical and technological perspectives.

Keywords: *Health monitoring, biosignals, vital signs, contactless, telemedicine, data fusion, computer vision, millimeter-wave radar*

Introduction

Vital signs, including heart rate (HR), respiratory rate (RR), blood pressure (BP), and body temperature (BT), are essential indications of physiological condition. Ongoing surveillance of these indicators facilitates the early identification of clinical situations, evaluation of disease progression, and direction for therapeutic actions. It also facilitates personal health monitoring in domains like as wellness and athletics, where users monitor performance and recuperation. Conventional measurement often depends on contact devices, such as hospital-based equipment that need skilled workers for data recording and interpretation. Progress in low-power electronics and wearable devices has facilitated continuous monitoring outside clinical environments, aiding daily health and fitness applications. Notwithstanding their advantages, wearables and other contact-based technologies exhibit limits, especially in certain applications like newborn care and burn units. Furthermore, prolonged use may induce pain, limit movement, and result in accuracy problems if the sensor location is inadequate. They need regular maintenance, hence escalating expenses in high-demand or resource-limited settings. User adherence and the longevity of gadgets may pose challenges in sporting or fitness environments. These issues have stimulated increasing interest in non-contact methodologies, including vision-based and radio frequency (RF)-based solutions. Vision-based methodologies use cameras to assess heart rate (HR) or respiratory rate (RR) via methods such as remote photoplethysmography (rPPG) or nuanced motion analysis. Despite being accessible and cost-effective, these approaches may be susceptible to variations in lighting conditions. RF methodologies, such mmWave radars and WiFi-based devices, use reflected signals to identify minor chest movements associated with cardiac and respiratory cycles. They function via clothes or bedding and are little impacted by variations in light, but they may be affected by substantial body movements. Integrating vision and RF data may effectively reconcile these trade-offs and improve overall performance. Figure 1 presents a comprehensive overview of various non-contact methodologies, while Figure 2

[1,2,3,4]*International School of Technology and Sciences for Women, A.P, India.*

illustrates the increasing research focus on multi-sensory vital sign analysis after 2020. Vital signs, such as breathing rate, heart rate, blood pressure, and body temperature, are essential indications for assessing an individual's physical condition. One. Irregular breathing and heart rates sometimes serve as preliminary signs of diverse ailments or health issues, including pulmonary diseases, cardiovascular conditions, and epileptic seizures. 2 to 4. Real-time monitoring of breathing and heart rate may enable early intervention, assist people in modifying their lifestyle, and enhance dietary and exercise practices, which are crucial for contemporary health and are garnering heightened focus. Respiration and heartbeat monitoring generally categorize into two types: contact and contactless. Traditional contact-based breathing and heartbeat monitoring technologies, such as the electrocardiograph (ECG), photoplethysmography (PPG), stethoscope, Chinese medicine pulse diagnostic, and wristwatch, encounter several challenges. For example, ECG and PPG need prolonged attachment of sensors to the skin, stethoscopes and traditional Chinese pulse diagnostic techniques are very labor-intensive, and the precision of heart rate monitoring by smartwatches requires enhancement. Camera-based and radar-based monitoring are two frequently used contactless techniques for assessing breathing and heart rate. Camera-based surveillance is not only affected by lighting conditions but also presents privacy problems. Radar-based monitoring broadcasts wideband radar waves to get high-precision range measurements and then use different algorithms to extract respiratory and cardiac rates. The precision of radar-based monitoring is directly correlated with the bandwidth of the radar signal; thus, to get high accuracy, a wide-bandwidth radar signal is essential. Unfortunately, the creation and processing of broadband radar signals are fundamentally constrained by technological bottlenecks.

To overcome the shortcomings of traditional contact monitoring devices, many optical fiber sensing systems have been suggested for physical state monitoring, leveraging their advantageous characteristics, including compactness, lightweight construction, and heightened sensitivity. 3.18–20. A wearable optical fiber sensing device integrates fiber Bragg grating (FBG) with a fiber laser sensor to assess several physiological parameters.

Principle and system

Figure 2 illustrates the schematic representation of the proposed seamlessly integrated contact and contactless vital sign monitoring system, enhanced by ROF support inside a WDM optical network. The vital sign monitoring system primarily comprises a central office and several user terminals interconnected via the WDM optical network. Each user terminal is equipped with one or both functionalities of FBG-based contact respiration and heartbeat monitoring and radar-based contactless respiration and heartbeat monitoring. Various techniques for monitoring breathing and heartbeat may be chosen based on the application context and the user's condition.

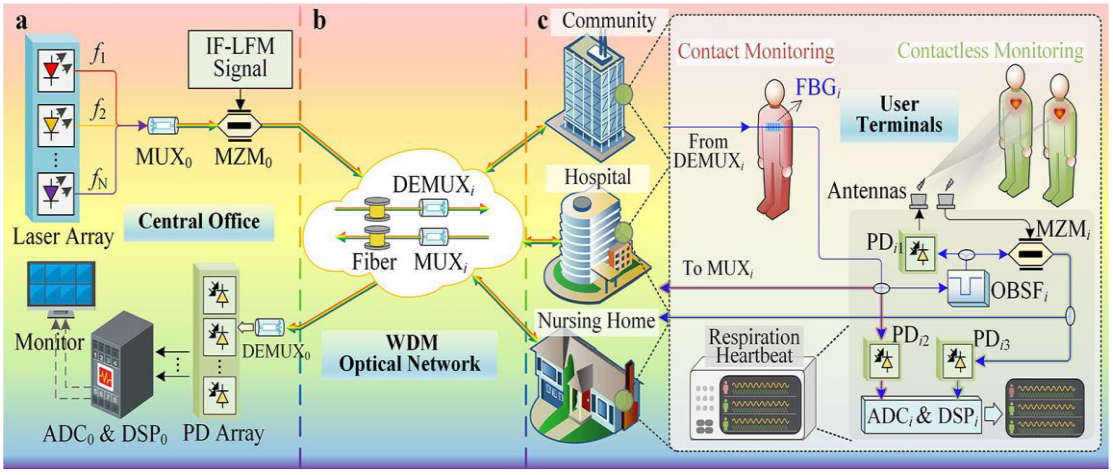

Fig. 2 Schematic diagram of the proposed seamlessly integrated contact and contactless vital sign monitoring system with ROF assistance incorporated in a WDM optical network.

a Headquarters. b Wavelength Division Multiplexing optical network. c User terminals. MUX: optical multiplexer; MZM: Mach–Zehnder modulator; DEMUX: optical demultiplexer; FBG: fiber Bragg grating; OBSF: optical band-stop filter; PD: photodetector; ADC: analog-to-digital converter; DSP: digital signal processing.
In the central office, as seen in Fig. 2a, several optical carriers (f1, f2, ···, fN), according to ITU WDM wavelength standards, are produced by a laser array and then introduced into a Mach–Zehnder modulator (MZM0) after wavelength multiplexing in an optical multiplexer (MUX0). In MZM0, each optical carrier is separately modulated by an intermediate frequency (IF)-linear frequency modulation (LFM) signal. The instantaneous frequency of the IF-LFM signal is expressed as $f_{IF}(t) = f_C - 0.5f_B + kt$, where f_C, f_B, and k represent the center frequency, bandwidth, and chirp rate of the IF-LFM signal, respectively. MZM0 is configured at the maximum transmission point (MATP) to ensure that each optical carrier is modulated only to generate the even-order optical sidebands of the IF-LFM signal. Under small-signal modulation conditions, only the original optical carriers and their ±2nd-order optical sidebands are considered, as seen in Fig. 3a. The many optical carriers, post-modulation in MZM0, are conveyed over an optical cable to various operational sites, including hospitals, nursing homes, and smart communities. An optical demultiplexer (DEMUX) is used at each operating site to segregate the various WDM channels, as seen in Fig. 2b. According to the distinct specifications of each user terminal for respiratory and cardiac monitoring, one or several wavelengths are sent to the user terminal via short optical fibers. The user terminal may be a consulting room or ward in a hospital, a bedroom or activity room in a nursing home, or a residence in a smart community. Following this short-distance fiber distribution, a minimum of one optical carrier centered at fi and its two ±2nd-order optical sidebands $f_i \pm (2f_C - f_B + 2kt)$ are used in a single user terminal.
Advanced Radar Techniques Utilizing Radar Technology.
Recent improvements in radar technology include the use of machine learning and signal processing methodologies to improve blood pressure estimate precision. Frequency Modulated Continuous Wave (FMCW) and Doppler radar systems have shown encouraging outcomes, using characteristics such as pulse amplitude, transit time, and body dimensions for estimate. Research has attained accuracy rates over 94% for systolic blood pressure (SBP) and diastolic blood pressure (DBP) with the use of machine learning algorithms. Dual radar systems enhance robustness by enabling the concurrent monitoring of several locations, hence refining PTT-based computations. High-frequency continuous wave radar (e.g., 300 GHz) has been investigated for enhanced spatial resolution and precision. Methods such as random forest algorithms and artificial neural networks have proven useful in blood pressure prediction by discerning intricate patterns in radar signal data.

Results

Experimental setup

A proof-of-concept experiment is conducted to illustrate the proposed seamlessly integrated contact and contactless vital sign monitoring system, using the configuration shown in Fig. 4. Two wavelengths are used in the experiment: one for contact-based respiration and heartbeat monitoring, and the other for concurrent contact and contactless respiration and heartbeat monitoring. Two continuous-wave (CW) laser sources (ID Photonics, CoBriteDX1-1-C-H01-FA and CoBriteDX1-1-HC1-FA) with central wavelengths of 1549.36 nm and 1549.92 nm, respectively, are used. Owing to the precision of FBG fabrication, the optical wavelengths chosen in the proof-of-concept experiment do not strictly adhere to the ITU WDM standard for optical wavelengths and spacing; however, this will not impede the validation of the method and concept illustrated in Fig. 2 through this experiment. The two optical wavelengths are merged in an optical coupler (OC1) after their passage via two polarization controllers (PC1 and PC2), which are used to modify their polarization states. The role of OC1 parallels that of the MUX seen in Fig. 2. Due to the absence of an appropriate MUX in the laboratory, OC1 is used as a replacement. The aggregated optical signal from OC1 is introduced into MZM0 (Fujitsu FTM7938EZ). MZM0 is powered by an IF-LFM signal with a 6.6-GHz central frequency and a 1-GHz bandwidth. The IF-LFM signal is produced by a microwave up-conversion module including an arbitrary waveform generator (AWG, Keysight M8190A), a microwave signal source (MSG, Agilent 83752B), a mixer (MITEQ M30), EA1 (CTT ALM/145-5023-293), and EBPF1 (KGL YA353-2). The modulated optical signal in MZM0

is sent by a 4.1-km optical cable and then bifurcated by OC2. The function of OC2 is anticipated to resemble that of the DEMUX seen in Fig. 2. Due to OC2's lack of filtering and wavelength selection capabilities found in the DEMUX, an extra optical filter is necessary to pick the appropriate wavelength when using its optical signal to create radar signals for non-contact respiration and cardiac monitoring. However, for contact respiration and heartbeat monitoring, filtering is unnecessary as FBG functions only at its designated wavelength.

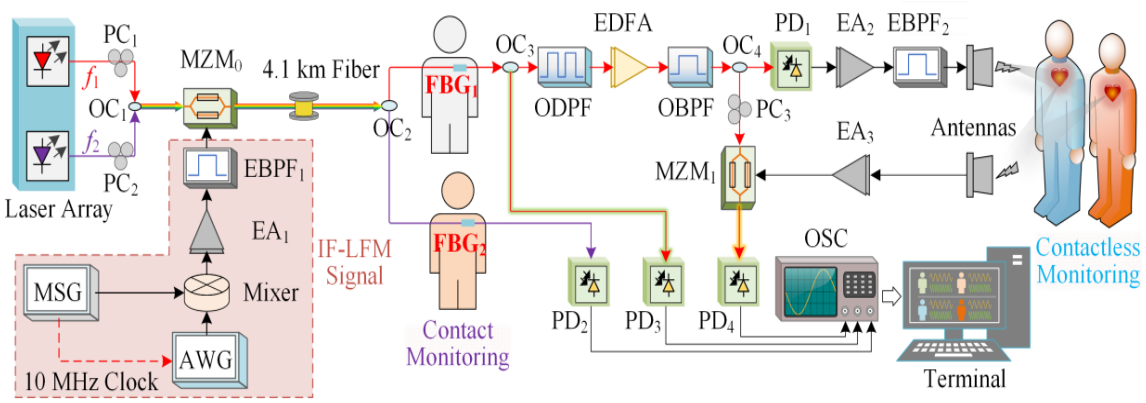

Fig. 4 Experimental setup of the contact and contactless vital sign monitoring system.

PC polarization controller, OC optical coupler, MZM Mach–Zehnder modulator, EBPF electrical band-pass filter, EA electrical amplifier, MSG microwave signal generator, AWG arbitrary waveform generator, FBG fiber Bragg grating, ODPF optical dual-passband filter, EDFA erbium-doped fiber amplifier, OBPF optical band-pass filter, PD photodetector, OSC oscilloscope.

The dual outputs of OC2 are sent to FBG1 and FBG2, which are touch sensors affixed to the human chest for measuring breathing and heartbeat. The transmission outputs from the two FBGs are detected by two low-speed photodetectors (PD2 and PD3, Beijing Lightsensing Technologies Ltd. BLPD-PFA1-60BR-W7) to translate optical power variations into the electrical domain. Simultaneous breathing and heartbeat monitoring of two individuals may be accomplished by evaluating the output power of the FBG. The output of FBG1 is bifurcated into two halves by OC3: One component is used for the previously described contact respiration and heartbeat monitoring; the other component is employed for future contactless respiration and heartbeat monitoring. The optical signal for non-contact breathing and heartbeat monitoring from OC3 is linked to an optical dual-passband filter (ODPF, Finisar WaveShaper 4000A). The ODPF operates as both the DEMUX in Fig. 2 to pick the appropriate WDM channel and the OBSF in Fig. 2 to attenuate the optical carrier. The ±2nd-order optical sidebands with frequency of f1 ± (2fC – fB + 2kt) are produced by the ODPF and then amplified by an erbium-doped fiber amplifier (EDFA, Amonics AEDFA-PA-35-B-FA) exhibiting a minor signal gain of 35 dB. The enhanced optical signal is sent to an optical band-pass filter (OBPF, EXFO XTM-50) to attenuate the amplified spontaneous emission (ASE) noise. The output optical signal from the OBPF is bifurcated into two pathways by OC4: One output of OC4 is directed into MZM1 (Fujitsu FTM7938EZ) to serve as an optical reference for radar de-chirping; the other output of OC4 is linked to high-speed PD1 (u2t MPRV1331A), where the two ±2nd-order optical sidebands interfere to produce a frequency-quadrupled LFM signal ranging from 24.4 GHz to 28.4 GHz. EA2 (CENTELLAX OA4MVM2) and EBPF2 (Shanghai AT Microwave AT-BPF-2432) are used to amplify signal power and mitigate interference and noise. The frequency-quadrupled LFM signal is emitted via a transmitting antenna for non-contact breathing and cardiac monitoring. The echo signal reflected from the human chest is captured by a receiving antenna and then amplified by EA3 (CENTELLAX OA4MVM3) with a gain of 27 dB. The optical reference is altered by the amplified echo signal at MZM1. Microwave photonic de-chirping is performed upon detection in low-speed PD4 (Nortel PP-10G). The radar de-chirped signal from PD4, together with the electrical signals from PD2 and PD3, are collected by a real-time oscilloscope (OSC, Rohde & Schwarz

RTO2032). Through the analysis of the radar de-chirped signal phase in Matlab, simultaneous contactless monitoring of breathing and heartbeat for numerous individuals may be accomplished.

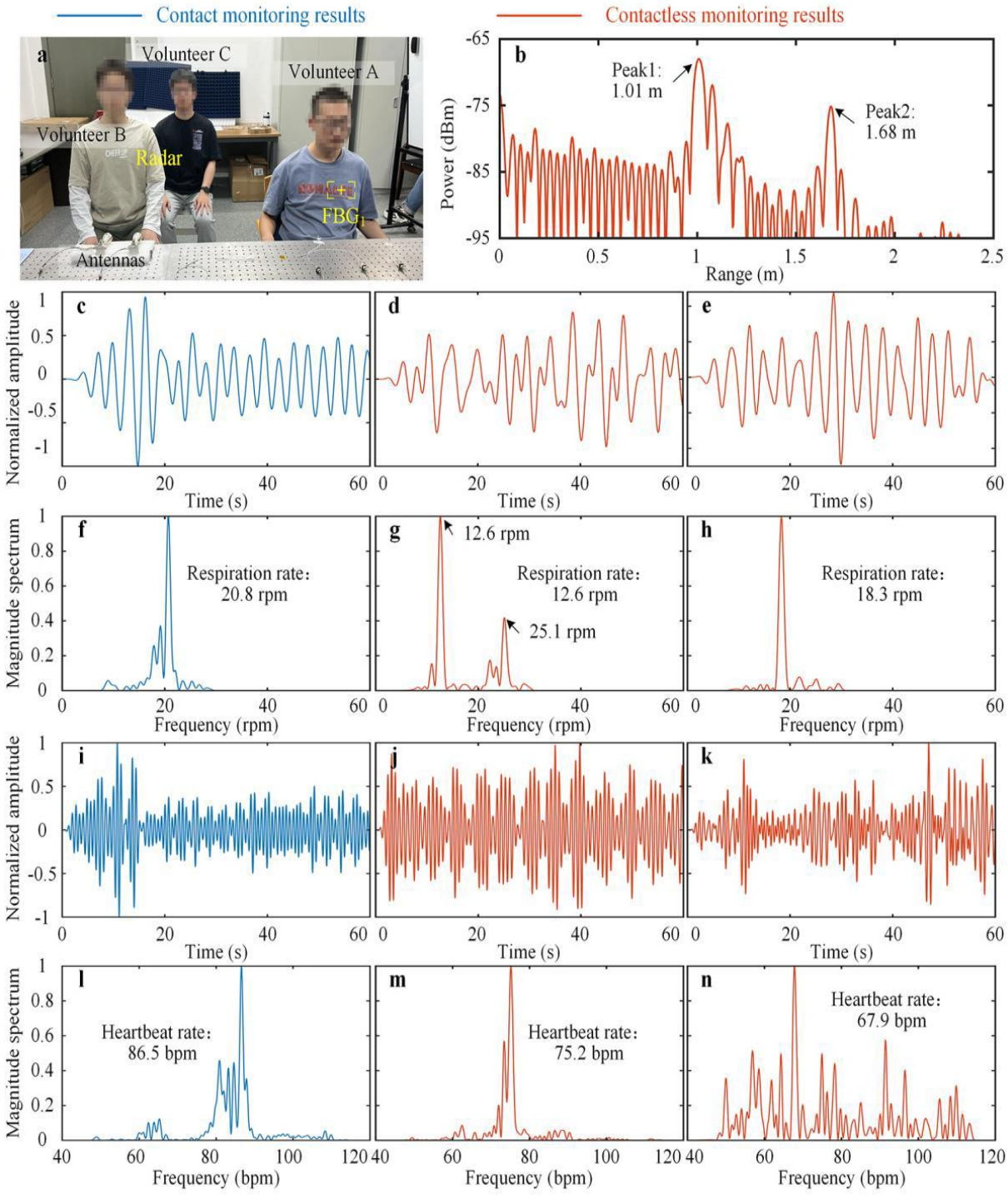

Fig. 6 Results of simultaneous contact and contactless vital sign monitoring using two channels.

a Three volunteers for both contact and contactless vital sign monitoring. b Range profile of Volunteers B and C derived from the radar de-chirped signal. C and F Respiration waveform and spectrum of Volunteer A: i and l Contact heartbeat waveform and spectrum of Volunteer A, d and g. Contactless respiratory waveform and spectrum of Volunteer B. j and m Contactless heartbeat waveform and

spectrum of Volunteer B, e, and h. Contactless respiratory waveform and spectrum of Volunteer C. k and n Contactless cardiac waveform and spectrum of Volunteer C.

Discussion

In the aforementioned respiration and heartbeat monitoring tests, the optical intensity of the FBG output and the radar de-chirped signal are sampled simultaneously at a duration of 60 seconds, indicating that users must allocate up to 60 seconds for monitoring. In several application contexts, it is very advantageous for monitoring to be executed more rapidly. A comprehensive analysis of the data is undertaken to examine the impact of sample time on the outcomes of breathing and cardiac monitoring. The two data sets corresponding to contact monitoring and contactless monitoring in Figures 5b and 5c are used. By intercepting sample signals of varying durations, namely 5 s, 10 s, 20 s, 30 s, 40 s, 50 s, and 60 s, we conduct a further analysis of the monitoring data corresponding to these distinct sampling intervals. The signal processing technique aligns with the aforementioned description. This research used the 3-dB bandwidth of the respiration and heartbeat signal spectra to denote respiration resolution and heartbeat resolution. Figures 8a and 8d illustrate contact respiration resolution and heartbeat resolution, while Figures 8b and 8e depict contactless measurements.

Respiratory resolution and cardiac resolution. It is noted that an increase in sample duration significantly enhances respiratory and heartbeat resolution. When the duration of sampling beyond 30 seconds, the resolution of breathing and heartbeat tends to stabilize. Figures 8c and 8f illustrate the observed and real values of respiration and heartbeat rates throughout various sample durations. While the monitoring resolution diminishes with a decrease in sample duration, this drop does not substantially affect the monitoring outcomes, since there is often just a single peak seen in the monitoring of respiration and heartbeat. The analysis and results indicate that the sampling duration of the proposed respiration and heartbeat monitoring system can be reduced to 5 seconds, thereby enhancing the system's efficiency and real-time performance.

Generation of broadband radar signals

The microwave up-conversion module is designed to produce an IF-LFM signal. The AWG generates a low-frequency LFM signal with a central frequency of 1.75 GHz, a bandwidth of 1 GHz, a pulse duration of 100 μs, and a pulse width of 60 μs. The low-frequency LFM signal is combined with a 13.5-dBm, 8.35-GHz local oscillator (LO) signal from the MSG, then amplified by EA1 and filtered by EBPF1. An IF-LFM signal with a 6.6-GHz center frequency and a 1-GHz bandwidth is produced and used with MZM0. Figure 9d illustrates the optical spectrum of the IF-LFM-modulated optical signal from MZM0. The frequency disparity between the two optical carriers is 70 GHz. The Bragg wavelength of FBG1 will change when the grating period and effective refractive index of FBG1 are modified owing to chest wall movement. By placing the optical wavelength, centered at 1549.36 nm, near the periphery of the transmission spectrum of FBG1, any movement of the chest wall would therefore induce a variation in the transmission power of FBG1. Figures 9e and 9f depict the optical spectra of the FBG1 output signal as the Bragg wavelength varies with the motion of the human chest wall. The intensity of the optical carrier at 1549.36 nm exhibits variations, while other components stay stable. An ODPF, shown in Fig. 9g, is used to select the ±2nd-order optical sidebands of the IF-LFM signal. The ODPF has a 3-dB bandwidth of 22.5 GHz, with the notch positioned at a wavelength of 1549.36 nm. The optical signal produced from the ODPF is amplified by the EDFA and filtered by the OBPF, serving as both the optical reference and the input signal for PD1. Figure 9h illustrates the optical spectrum of the input signal of PD1. Only two ±2nd-order optical sidebands are detected, but the optical carrier in this channel and the optical signal in the alternative channel are significantly attenuated. Upon detection of the optical signal seen in Fig. 9h by PD1, amplification occurs in EA2, followed by filtration in EBPF2, resulting in the electrical spectrum of the produced radar signal illustrated in Fig. 9i. Unlike the IF-LFM signal, the transmitted radar signal has a fourfold increase in both its center frequency and bandwidth, including a center frequency of 26.4 GHz and a bandwidth of 4 GHz.

Contact and contactless signal sampling

The suggested vital sign monitoring system may concurrently provide both touch and contactless monitoring of breathing and heartbeat. The

experiment employs a microwave up-conversion module to produce the IF-LFM signal, characterized by a central frequency of 6.6 GHz, a bandwidth of 1 GHz, a pulse time of 100 μs, and a pulse width of 60 μs. A 10-MHz sinusoidal signal from MSG is sent to the AWG for signal synchronization. The movement of the chest wall due to breathing and heartbeat in FBG-based monitoring immediately corresponds with fluctuations in the optical intensity of the FBG output, which is then transferred to the electrical domain via PD2 and PD3. The outputs of PD2 and PD3 are sampled by the OSC at a rate of 50 Sa/s throughout the experiment. The waveforms are further analyzed in the digital domain to ascertain the breathing and heartbeat rates. The transmitted radar signal used in radar-based contactless respiration and heartbeat monitoring is a broadband LFM signal produced from 24.4 GHz to 28.4 GHz. The radar de-chirped signal is derived from photonic frequency mixing in PD4 and sampled with the OSC at a rate of 10 MSa/s. By examining the phase of the radar de-chirped signal, respiratory and cardiac rates may be derived in non-contact monitoring. It is important to acknowledge that in contactless monitoring, the high sampling rate of the de-chirped radar signal may lead to complications such as an overwhelming volume of sampled data and reduced processing rates if direct sampling is used. Due to the gradual changes in breathing and heartbeat rates, it is unnecessary to sample all radar de-chirped waveforms for the whole duration of sampling. This may significantly decrease the volume of sampled data and enhance processing velocity. A rectangular pulse signal with a duration of 20 ms and a width of 60 μs is attached to the external trigger port of the oscilloscope to facilitate intermittent signal sampling. The rectangular pulse is created straight from the AWG in this experiment. In practical applications, the rectangular pulse may be locally produced at the user terminal by a pulse generator.

Conclusion

Our findings indicate that the economical 24 GHz FMCW radar, along with the suggested vital sign extraction techniques, offers a reliable option for nocturnal vital sign monitoring across diverse situations, including sleep apnea. We achieved cutting-edge accuracy in heart rate monitoring and, to our knowledge, are the first to report minimal mistakes in capturing instantaneous interbeat intervals with a comparable technology [4]. Furthermore, we established the radar's viability in the analysis of heart rate variability. Ultimately, we delivered very precise outcomes in respiration monitoring, sustaining an acceptable margin of error from unusually shallow breathing to high-volume gasping. This research seems to be the inaugural investigation using atypically little respiratory movements within the analyzed respiratory range and assessing FMCW radar technology for apnea detection.

Although our research concentrated on nighttime vital sign monitoring applications, the technique is also relevant to many other contexts where people stay mostly stationary, such as monitoring bedridden patients or the elderly, or locating victims buried under debris in disaster scenarios.

In the future, the techniques may be evaluated using genuine nighttime data and refined for more sophisticated 60 GHz radars, enabling the simultaneous assessment of numerous participants in close proximity [35]. Additional persistent issues include mitigating the impact of motion artifacts and minimizing the time lag in signal extraction to facilitate real-time applications.

References

1. Ludikhuize, J., Smorenburg, S. M., de Jonge, S. E. & de Jonge E. Identification of deteriorating patients on general wards; measurement of vital parameters and potential effectiveness of the Modified Early Warning Score. *J. Crit. Care* **27**, 424.e7–424.e13 (2012).

2. Barfod, C. et al. Abnormal vital signs are strong predictors for intensive care unit admission and in-hospital mortality in adults triaged in the emergency department - a prospective cohort study. *Scand. J. Trauma Resus. Emerg. Med.* **20**, 28 (2012).

3. Massaroni, C. et al. Fiber Bragg grating sensors for cardiorespiratory monitoring: A review. *IEEE Sensors J.* **21**, 14069–14080 (2021).

4. Lotufo, P. A., Valiengo, L., Benseñor, I. M. & Brunoni, A. R. A systematic review and meta-analysis of heart rate variability in epilepsy and antiepileptic drugs. *Epilepsia* **53**, 272–282 (2012).

5. Schläpfer, J. & Wellens, H. J. Computer-interpreted electrocardiograms: Benefits and limitations. *J. Am. Coll. Cardiol*. 70, 1183–1192 (2017).

6. Lan, K., Raknim, P., Kao, W. & Huang, J. Toward hypertension prediction based on PPG-derived HRV signals: a feasibility study. *J. Med. Syst.* **42**, 103 (2018).

7. King, C. E. & Sarrafzadeh, M. A survey of smartwatches in remote health monitoring. *J. Healthc. Inform. Res*. **2**, 1–24 (2018).

8. Molinaro, N. et al. Contactless vital signs monitoring from videos recorded with digital cameras: An overview. *Front. Physiol.* **13**, 801709 (2022).

9. Selvaraju, V. et al. Continuous monitoring of vital signs using cameras: A systematic review. *Sensors* **22**, 4097 (2022).

10. Paterniani, G. et al. Radar-based monitoring of vital signs: A tutorial overview. *Proceedings of the IEEE* **111**, 277–317 (2023).

11. Kebe, M. et al. Human vital signs detection methods and potential using radars: A review. *Sensors* **20**, 1454 (2020).

12. Aarts, L. A. M. et al. Non-contact heart rate monitoring utilizing camera photoplethysmography in the neonatal intensive care unit — A pilot study. *Early Hum. Dev.* **89**, 943–948 (2013).

13. Park, B. K., Lubecke, O. B. & Lubecke, V. M. Arctangent demodulation with DC offset compensation in quadrature Doppler radar receiver systems. *IEEE Trans. Microw. Theory Tech.* **55**, 1073–1079 (2007).

14. Mercuri, M. et al. Vital-sign monitoring and spatial tracking of multiple people using a contactless radar-based sensor. *Nat. Electron.* **2**, 252–262 (2019).

15. Park, J. et al. Preclinical evaluation of noncontact vital signs monitoring using real-time IR-UWB radar and factors affecting its accuracy. *Sci. Rep.* **11**, 23602 (2021).

16. Shi, K. et al. Contactless analysis of heart rate variability during cold pressor test using radar interferometry and bidirectional LSTM networks. *Sci. Rep.* **11**, 3025 (2021).

17. Ghelfi, P. et al. Photonics in radar systems: RF integration for state-of-the-art functionality. *IEEE Microw. Mag.* **16**, 74–83 (2015).

18. Rohan, R., Venkadeshwaran, K. & Ranjan, P. Recent advancements of fiber Bragg grating sensors in biomedical application: a review. *J. Opt.* **53**, 282–293 (2023).

19. Zhao, Y., Lin, Z., Dong, S. & Chen, M. Review of wearable optical fiber sensors: Drawing a blueprint for human health monitoring. *Opt. Laser Technol.* **161**, 109227 (2023).